

# Carrot mottle virus ORF4 movement protein targets plasmodesmata by interacting with the host cell SUMOylation system

Jun Jiang<sup>1</sup> , Yen-Wen Kuo<sup>1</sup> , Nidà Salem<sup>2</sup> , Anna Erickson<sup>1</sup>  and Bryce W. Falk<sup>1</sup> 

<sup>1</sup>Department of Plant Pathology, University of California, Davis, CA 95616, USA; <sup>2</sup>Department of Plant Protection, School of Agriculture, The University of Jordan, Amman 11942, Jordan

## Summary

Author for correspondence:  
Bryce W. Falk  
Email: [bwfalk@ucdavis.edu](mailto:bwfalk@ucdavis.edu)

Received: 8 February 2021

New Phytologist (2021)  
doi: 10.1111/nph.17370

**Key words:** *Carrot mottle virus* (CMoV), movement proteins (MPs), plasmodesmata (PD), small ubiquitin-like modifier (SUMO), *Umbravirus*.

- Plant virus movement proteins (MPs) facilitate virus spread in their plant hosts, and some of them are known to target plasmodesmata (PD). However, how the MPs target PD is still largely unknown.
- *Carrot mottle virus* (CMoV) encodes the ORF3 and ORF4 proteins, which are involved in CMoV movement. In this study, we used CMoV as a model to study the PD targeting of a plant virus MP.
- We showed that the CMoV ORF4 protein, but not the ORF3 protein, modified PD and led to the virus movement. We found that the CMoV ORF4 protein interacts with the host cell small ubiquitin-like modifier (SUMO) 1, 2 and the SUMO-conjugating enzyme SCE1, resulting in the ORF4 protein SUMOylation. Downregulation of mRNAs for NbSCE1 and NbSUMO impaired CMoV infection. The SUMO-interacting motifs (SIMs) LVIVF, VIWV, and a lysine residue at position 78 (K78) are required for the ORF4 protein SUMOylation. The mutation of these motifs prevented the protein to efficiently target PD, and further slowed or completely abolished CMoV systemic movement.
- Finally, we found that some of these motifs are highly conserved among umbraviruses. Our data suggest that the CMoV ORF4 protein targets PD by interacting with the host cell SUMOylation system.

## Introduction

To establish multicellular infections, plant virus infections spread from initially infected to neighboring cells via modified plasmodesmata (PD) (cell-to-cell movement), and further load into the vascular tissues (long-distance movement). These processes are facilitated by virus-encoded movement proteins (MPs). The 30 kilodalton (30K) protein of *Tobacco mosaic virus* (TMV), the 3a protein of *Cucumber mosaic virus* (CMV), and the triple gene block proteins (TGBs) of *Potato virus X* (PVX) are typical virus MPs (Demo *et al.*, 1987; Ding *et al.*, 1995; Tilsner *et al.*, 2013). A single MP, such as the TMV 30K protein or the CMV 3a protein, can bind to the viral ribonucleoprotein complexes (RNPs), and promote their cell-to-cell movement (Ding *et al.*, 1995; Kawakami *et al.*, 2004). For many other viruses, cooperation of multiple MPs is required for their cell-to-cell movement. In the case of PVX, the TGB1 coordinates with the TGB2-derived granular vesicles, to which TGB3 is recruited during infection, for their cell-to-cell movement (Tilsner *et al.*, 2012). All of these MPs are known to increase the size exclusion limit of PD (Wolf *et al.*, 1989; Vaquero *et al.*, 1994; Angell *et al.*, 1996; Su *et al.*, 2010). Alternatively, many MPs can physically damage the PD by lining its interior. For example, the MPs of *Cowpea mosaic*

*virus* (CPMV) and *Cauliflower mosaic virus* (CaMV) can induce tubules that traverse the PD, allowing for cell-to-cell movement of their virions (Kasteel *et al.*, 1996). These MPs can bind to the host cell cytoskeleton, including microfilaments and microtubules, to efficiently relocate to the PD (Ashby *et al.*, 2006; Brandner *et al.*, 2008; Su *et al.*, 2010). Meanwhile, these MPs can sever or reorganize the cytoskeleton to increase the size exclusion limit of PD (Su *et al.*, 2010).

There are only a few cases in which the mechanisms of how MPs target PD are known. One example is the TMV 30K protein, which interacts with the host cell protein synaptotagmin A (SYTA) through the N-terminal 50 amino acid residues of the 30K protein to target PD (Yuan *et al.*, 2018). In the case of *Fig mosaic virus* (FMV), two different cellular routes have been proposed to illustrate how its MP reaches the PD. The MP N-terminal signal peptide directs the protein to the endoplasmic reticulum (ER)–plasma membrane (PM) contact site, while the remainder of the FMV MP is transferred to the PM microdomain, and both further reach the PD (Ishikawa *et al.*, 2017). Interestingly, the MP of *Citrus psorosis virus* (CPsV) can be autocleaved to release the N-terminal 34 kDa protein, to target PD and induce the formation of tubules that support intercellular movement (Robles Luna *et al.*, 2018).

Post-translational modifications of proteins also have been shown to regulate virus cell-to-cell movement (Waigmann *et al.*, 2000; Hu *et al.*, 2015). SUMOylation is one kind of post-translational modification that leads to the conjugation of small ubiquitin-like modifier (SUMO) to the target protein (Morrell & Sadanandom, 2019). Different from ubiquitination, SUMOylation can sequester the lysine residues that are prone to ubiquitin-mediated protein degradation, thus protecting them from degradation. SUMOylation is a rapid and reversible process, involving activation, conjugation and ligation steps. Initially, the extended C-terminus of the SUMO precursor is cleaved by deSUMOylating proteases to expose the C-terminal Gly-Gly motif. The SUMO is activated by the E1 heterodimer SUMO activating enzyme subunit 1/2 (SAE1/2), and is transferred to the E2 SUMO-conjugating enzyme 1 (SCE1), and is then donated to the lysine residue(s) within the target protein (Augustine & Vierstra, 2018). The SUMO is preferentially conjugated to the lysine residue within the consensus SUMOylation motif (the motif is defined as  $\Psi$ KXD/E, where  $\Psi$  is a hydrophobic amino acid and X may be any amino acid). SUMOylation can alter protein cellular localization, block protein–protein interactions, and promote the formation of complexes (Wilson & Rangasamy, 2001). The protein–protein interaction can occur via a noncovalent bond that forms between proteins harboring a SUMO-interacting motif (SIM). SIMs are characterized by a short stretch of hydrophobic amino acids that are often flanked by acidic amino acid residues, such as the motif (V/I)X(V/I)(V/I) (Kerscher, 2007; Gareau & Lima, 2010). Host cell SUMOylation components, SCE1 and SUMO3, are known to interact with virus-encoded proteins. One example is the RNA-dependent RNA polymerase (RdRp) of *Turnip mosaic virus* (TuMV) where SUMOylation has been shown to be required for virus infection (Xiong & Wang, 2013; Cheng *et al.*, 2017). For the *Begomovirus*, *Tomato golden mosaic virus* (TGMV), the viral protein AC1 interacts with the host cell SCE1 protein, and this interaction is shown to be indispensable for virus infection (Sánchez-Durán *et al.*, 2011). Whether SUMOylation or SUMO interaction plays any role in plant virus movement is still unknown.

*Carrot mottle virus* (CMoV) is a positive-sense RNA virus that belongs to the genus *Umbravirus* in the family *Tombusviridae*. The viral genome, *c.* 4200 nt in length, has four open reading frames (ORFs) (Fig. 1). The two ORFs (ORF1 and ORF2) at the 5' end of the viral RNA (vRNA) are expressed by a  $-1$  frameshift to yield the viral RdRp. The other two ORFs, ORF3 (P26 in the case of *Pea enation mosaic virus-2* (PEMV2)) and ORF4 (P27 in the case of PEMV2), are overlapping. It has been shown that the ORF3 and ORF4 proteins are required for virus long-distance and cell-to-cell movement, respectively, for the *Umbravirus*, *Groundnut rosette virus* (GRV). The GRV ORF3 protein can bind the vRNA and form the RNPs, enabling virus systemic infection (Taliensky *et al.*, 2003; Kim *et al.*, 2007a; Kim *et al.*, 2007b; Canetta *et al.*, 2008). The ORF4 protein can induce tubular structures that protrude from the surface of the protoplasts, and this protein can functionally complement cell-to-cell movement of MP-deficient CMV (Ryabov *et al.*, 1999a; Nurkiyanova *et al.*, 2001). However, whether this is the case for

other umbraviruses, and the molecular determinants of the ORF4 protein PD targeting is unknown.

In this study, we showed that the CMoV ORF4 protein targets PD and induces tubule formation *in planta*. The ORF4 protein, but not the ORF3 protein, increased the size exclusion limit of PD, and supported the virus movement. The lysine residue at position 78 (K78) and the SIMs (LVIVF and VIWV) are required for efficient targeting of PD by the ORF4 protein, and mutation of these motifs either delayed or abolished the virus movement. We further demonstrated that the ORF4 protein interacts with host SUMOylation components SCE1, SUMO1 and SUMO2, but not SUMO3 and SUMO5, and this interaction led to the SUMOylation of the ORF4 protein. The characterized motifs, K78, LVIVF and VIWV, are required for efficient SUMOylation of the ORF4 protein, and the host cell SUMOylation components SCE1, SUMO1 and SUMO2 are required for efficient virus infection. Comparison of the ORF4 proteins encoded by other viruses of the genus *Umbravirus* suggests that this might also be the case for other *Umbravirus* ORF4-encoded proteins.

## Materials and Methods

### Plasmid construction

Unless otherwise noted, all constructs made in this work were generated using the Gibson Assembly<sup>®</sup> Master Mix (NEB, Ipswich, MA, USA) following the manufacturer's instructions. To make the construct pEAQ-HT/GFP:ORF4, the coding sequences of GFP and ORF4 were amplified by PCR using the construct pEAQ-HT/P26:GFP (Qiao *et al.*, 2018) and the pJL89/CMoV infectious clone (N. Salem, unpublished) as the template, respectively. The binary vector pEAQ-HT (Sainsbury *et al.*, 2009) was digested with *Nru*I and *Stu*I. The positive colonies were then confirmed by DNA sequencing. The construct, pEAQ-HT/ORF4:GFP, was constructed in a similar way. The ORF4 mutants were made by introducing either the mutations into the forward primer or the complementary mutations in the primers at the overlap region (see Supporting Information Table S1). To make the construct pJL89//CMoV ORF1/2:GFP, the overlapping sequences of ORF3/4 were replaced with the coding sequence of green fluorescent protein (GFP).

To make the construct pEAQ-HT/ntGFP and pEAQ-HT/ctGFP, the coding sequences of ntGFP and ctGFP were amplified by PCR using the pEAQ-HT/P26:GFP as the template; the fragments were then inserted into the vector pEAQ-HT which was digested with *Nru*I and *Stu*I. Similarly, to make the construct pEAQ/ORF4:ntGFP and pEAQ/ORF4:ctGFP, the coding sequences of ORF4, ntGFP and ctGFP were amplified using pJL89/CMoV or pEAQ-HT/P26:GFP as the template. To make the mutated pEAQ/ORF4:ntGFP constructs, the same steps were followed as described earlier, except that the mutated ORF4 coding sequences were amplified from their corresponding mutated ORF4:GFP constructs. The coding sequences of AtSCE1 (AT3G57870), AtSUMO1 (AT4G26840), AtSUMO2

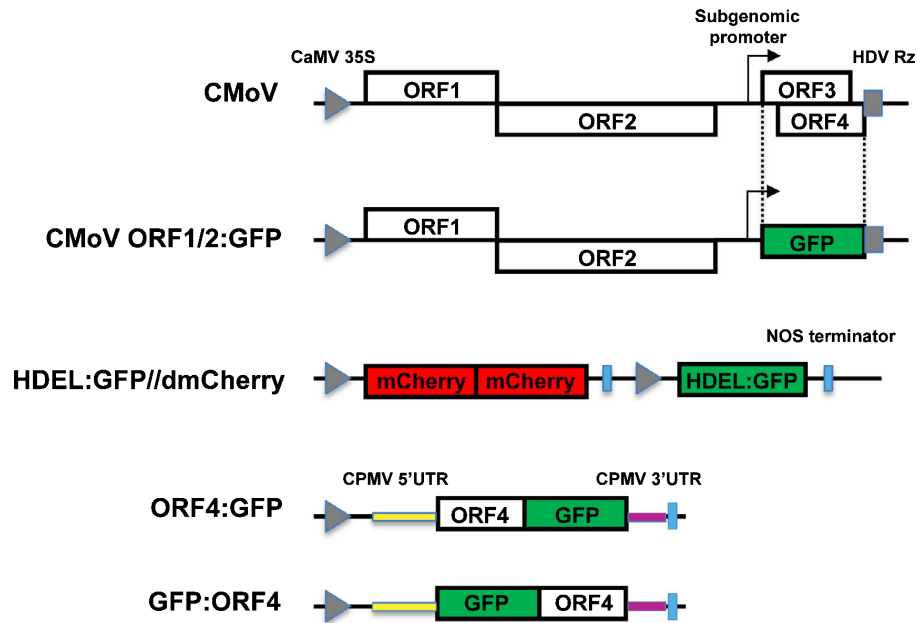


**Fig. 1** Schematic representation of the main constructs used in this study. At the top, the *Carrot mottle virus* (CMoV) genome is presented. To make the CMoV infectious clone, the CMoV genome was inserted into the binary vector pJL89. The gray triangles represent the *Cauliflower mosaic virus* (CaMV) 35S promoter, the gray bars represent the self-cleaving ribozyme sequence of the *Hepatitis D virus* (HDV), and the rectangles represent the open reading frames (ORFs). The CMoV subgenomic promoters are highlighted by the arrows. To make the construct CMoV ORF1/2:GFP, the ORF3/4 coding sequences were replaced with the GFP coding sequence. To express the ORF4:GFP and GFP:ORF4 fusion proteins, the coding sequences were inserted into the binary vector pEAQ-HT, and right between the *Cowpea mosaic virus* (CPMV) 5' untranslated region (5' UTR) and 3' UTR sequences.

(AT5G55160), AtSUMO3 (AT5G55170) and AtSUMO5 (AT2G32765) were amplified from the *Arabidopsis thaliana* (Col-0) cDNA. These fragments were then inserted into the backbone pEAQ-HT/ctGFP to generate the corresponding N-terminal ctGFP fusions.

To make the mutated CMoV infectious clones, a similar strategy to that used to make the mutated ORF4:GFP was adopted. Two fragments, one upstream and the other downstream of the mutation site, were amplified using the infectious clone pJL89/CMoV as the template. These fragments were then inserted into the backbone pJL89/CMoV which had been digested with *FspI* and *HpaI*. To make the construct pdM/ORF4:Myc, the ORF4 coding sequence was amplified using pJL89/CMoV as the template, and was then inserted into the vector pdM. The resulting pdM/ORF4:Myc and the vector pART27 were then digested with *NotI*, and the resulting construct was pART27/ORF4:Myc. To make the pART27/ORF4:Myc mutants, the ORF4 coding sequences were amplified using the corresponding ORF4:GFP mutant as the template. For more information, see Methods S1.

### Protein expression and virus inoculation

Protein transient expression was performed as described previously (Sparkes *et al.*, 2006). *Agrobacterium tumefaciens* GV3101 containing a recombinant expression plasmid was selected on LB kanamycin-rifampicin or spectinomycin agar plates. The positive colonies were then liquid-cultured overnight. The bacterial cultures were centrifuged and resuspended in water supplemented

with 10 mM MgCl<sub>2</sub> and 150 μM acetosyringone, and incubated at room temperature for 2–4 h. For transient expression, the optical density at 600 nm (OD<sub>600</sub>) was adjusted to 0.3 for all cultures, except to 0.1 for ERD2:GFP (Saint-Jore *et al.*, 2002) and GFP. Equal volumes of *A. tumefaciens* suspensions were mixed thoroughly when protein coexpression was needed. For *Tobacco rattle virus* (TRV) silencing, the OD<sub>600</sub> was adjusted to 1.0 for both TRV1 and TRV2 *A. tumefaciens* suspensions. The lower leaves were agroinfiltrated with the *A. tumefaciens* suspension mixture, and the plants were then kept in a growth chamber (24°C, 16 h : 8 h, light : dark) for 1 wk. The upper leaves were then agroinfiltrated with *A. tumefaciens* containing pJL89/CMoV infectious clone. The plants were then kept in the growth chamber (19°C, 16 h : 8 h, light : dark) until analysis.

### Confocal microscopy

Leaf sections (*c.* 1 × 1 cm) of agroinfiltrated *N. benthamiana* were imaged using Leica TCS SP8 inverted confocal microscopy with a ×20 objective or ×63 water immersion objective. GFP was excited at 488 nm, and the emission light was captured at 500–535 nm; mCherry was excited at 561 nm, and the emission light was captured at 580–640 nm. IMAGEJ was used to quantify the fluorescence intensity.

### Coimmunoprecipitation and Western blotting

*Nicotiana benthamiana* leaf tissues expressing the desired proteins were homogenized in liquid nitrogen, mixed with two volumes

of protein extraction buffer (100 mM Tris-HCl, pH 7.5; 100 mM EDTA, pH 8.0; 5 mM dithiothreitol; 150 mM NaCl; 0.1% Triton X-100; Cocktail proteinase inhibitor), and were then shaken constantly at 4°C for 30 min. The mixtures were centrifuged at 20 000 *g* for 15 min at 4°C, and the supernatant was then used for coimmunoprecipitation. Coimmunoprecipitation was done using the GFP-Trap resin (Chromotek, Planegg-Martinsried, Germany), following the manufacturer's instructions. Protein samples were separated with 12% polyacrylamide gel, and then transferred to a nitrocellulose membrane. The antisera were used at the following dilutions: anti-GFP (Invitrogen, Carlsbad, CA, USA) at 1 : 2000, anti-Myc (Miltenyi Biotec, Sunnyvale, CA, USA) at 1 : 5000, anti-T7 tag Antibody HRP conjugate (Novagen, La Jolla, CA, USA) at 1 : 5000.

### *E. coli* in vivo SUMOylation assay

The *E. coli* in vivo SUMOylation assay was done as described by Okada *et al.* (2009). The three plasmids, including the pACYC/SAE2-SAE1b and pCDF/SUMO1(GG)-SCE1a that encode the SUMOylation components, and the pET28a(+)/MYB30, the wild-type (WT) or mutated pET28a(+)/ORF4 that expresses the target protein, were cotransformed into the *E. coli* BL21(DE3) competent cells. For the negative controls, the plasmid pCDF/SUMO1(AA)-SCE1a was cotransformed instead. The presence of the three plasmids in the transformed *E. coli* was confirmed by PCR. The transformed cells were then cultured in 5 ml of LB medium at 37°C until the OD<sub>600</sub> was 1.0, followed by the addition of 1 mM isopropyl β-D-1-thiogalactopyranoside. After incubation at 25°C for 12 h, cells were harvested from 500 μl of cell culture, the pellet was resuspended with 100 μl 1 × sodium dodecyl sulfate-polyacrylamide gel electrophoresis sample buffer, followed by denaturation at 95°C for 5 min.

## Results

### CMoV ORF4 protein localizes to, induces tubule formation at, and modifies the PD

Previous studies showed that the ORF4 protein for the related *Umbravirus*, GRV, localized to the PD and induced tubular structures that protrude from the surface of protoplasts (Ryabov *et al.*, 1998; Nurkiyanova *et al.*, 2001). To determine if CMoV ORF4 protein induces similar structures and if they are generated *in planta*, constructs were made to express the green fluorescent protein (GFP) fused to the N-terminus and C-terminus of the CMoV ORF4 protein, and the resulting protein fusions, GFP:ORF4 and ORF4:GFP, were transiently expressed in leaves of the model plant *N. benthamiana*. As early as 24 h after agroinfiltration, the GFP:ORF4 fusion protein mostly accumulated as punctate structures along the cell periphery, and became more obvious at 48 and 72 h after agroinfiltration (Fig. 2a, left panels). The size of the punctate structures was estimated to be  $0.77 \pm 0.28 \mu\text{m}$  ( $n = 45$ ), and did not change significantly over the time course examined. The ORF4:GFP fusion protein similarly mostly localized to the cell periphery (Fig. 2a, right panels).

However, rather than appearing as punctate structures, it appeared as extended tubules that crossed into adjacent cells. The length of those tubules was estimated to be  $1.94 \pm 0.60 \mu\text{m}$  ( $n = 45$ ) at 24 h after agroinfiltration, and increased to  $2.77 \pm 0.51 \mu\text{m}$  ( $n = 45$ ) at 72 h after agroinfiltration. We also found that both the GFP:ORF4 and ORF4:GFP proteins localized to the nucleus, cytoplasm and PM to a lesser extent (data not shown). To demonstrate those were truly tubules, the protoplasts were isolated from the leaf tissues expressing the GFP:ORF4 and ORF4:GFP fusion proteins. Clearly, tubules protruded from the surface of ORF4:GFP-expressing protoplasts, while no tubules were observed when GFP:ORF4 was expressed (Fig. 2a, lowest panels). To confirm that both fusion proteins localized to the PD, GFP:ORF4 and ORF4:GFP were coexpressed with the PD marker TMV MP:red fluorescent protein (RFP) fusion MP:RFP (Atkins *et al.*, 1991). Both the GFP:ORF4- and ORF4:GFP-induced structures that overlapped with MP:RFP (Fig. 2b). However, the size of MP:RFP-labeled PD appeared to be larger in the presence of ORF4:GFP, when compared with the empty vector and GFP:ORF4. To further confirm the PD localization of ORF4 protein, a subcellular fractionation assay was performed (Donald *et al.*, 1993). This allowed us to isolate proteins that are soluble (S30 fraction), membrane-associated (P30 fraction) and cell wall-associated (CW fraction). If the protein is localized to PD, then we expect the presence of this protein in the CW fraction. On the contrary, the presence of the protein in the CW fraction does not necessarily mean it is localized to the PD. The membrane-associated Golgi marker ERD2:GFP protein was present in the P30 fraction, the soluble protein GFP was found only in the S30 fraction, and neither was present in the CW fraction (Fig. 2c). The *A. thaliana* Plasmodesmata-Localized Protein 1 (AtPDLP1):GFP fusion (AtPDLP1:GFP) was used as the positive control. The presence of AtPDLP1:GFP in the CW fraction (Fig. 2c) confirmed the validity of this fractionation assay. As expected, both GFP:ORF4 and ORF4:GFP were present in the CW fraction (Fig. 2c). Overall, these results indicate that ORF4 protein can target to and induce the formation of tubules at the PD.

To determine if the ORF4 protein can increase the size exclusion limit of PD, we engineered a dual fluorescent protein-tagged reporter HDEL:GFP//dmCherry (Fig. 1). This construct expresses a HDEL:GFP fusion protein that is retained in the ER (Denecke *et al.*, 1992), thus labeling the agroinfiltrated cells, and the double mCherry fusion protein (57.6 kDa) that will diffuse into the adjacent cells only when the size exclusion limit of the PD is increased (Sakulkoo *et al.*, 2018). To coexpress with the reporter HDEL:GFP//dmCherry, constructs were made to express the nonfluorescent Myc tag separately to the C-termini of the ORF3 and ORF4 proteins. The resulting protein fusions are ORF3:Myc and ORF4:Myc, respectively. *Nicotiana benthamiana* leaf tissues expressing HDEL:GFP//dmCherry in the presence of empty vector, ORF3:Myc and ORF4:Myc were examined by confocal microscopy. When the empty vector or ORF3:Myc was coexpressed with HDEL:GFP//dmCherry, all the agroinfiltrated cells expressed both GFP and mCherry (Fig. 2d). However, cells showing only mCherry were found in the presence of ORF4:Myc



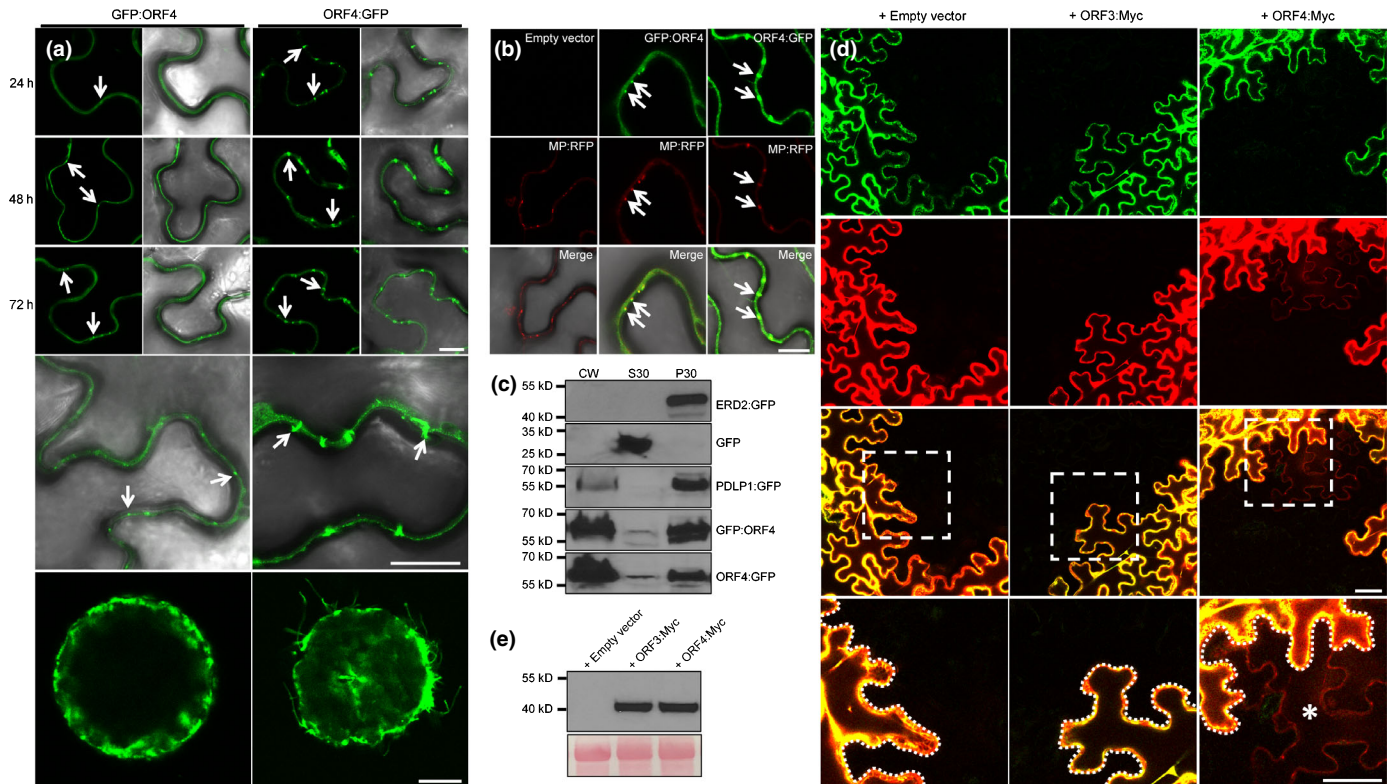


**Fig. 2** Subcellular localization of the transiently expressed ORF4 and green fluorescent protein (GFP) fusions. *Nicotiana benthamiana* leaf tissues expressing GFP:ORF4 or ORF4:GFP alone, observed at 24, 48 and 72 h after agroinfiltration (a), or coexpressed with *Tobacco mosaic virus* (TMV) movement protein:red fluorescent protein (MP:RFP) and checked 72 h later (b). In order to show the finer details, enlarged sections are shown at the bottom. The lowest panels show the protoplasts isolated from the agroinfiltrated *N. benthamiana* leaf tissues as observed by confocal microscopy 40 h later (a). (c) Cellular fractionation of ERD2:GFP, GFP, PDL1:GFP, GFP:ORF4 and ORF4:GFP. Cell wall (CW), supernatant (S30) and 30 000 × g pellet (P30), were analyzed by immunoblot using antibodies against GFP. (d) *Nicotiana benthamiana* leaf tissues expressing empty vector, ORF3:Myc and ORF4:Myc, together with the reporter HDDEL:GFP//dmCherry. Proteins were extracted from the agroinfiltrated leaf tissues and subjected to immunoblot using anti-Myc antibodies (e). The Ponceau S stained Rubisco large subunit serves as a loading control. The GFP channels are shown on the left (a) or at the top (b, d), the red channels are shown in the middle (b, d), with merged panels shown on the right (a) or at the bottom (b, d). The areas outlined by the white boxes are enlarged in the lowest panels (d). The arrows in (a) and (b) indicate the plasmodesmata (PD), and the star in (d) highlights the cell that showing mCherry only. Bars: (a, b) 20 μm; (d) 50 μm.

(Fig. 2d). In this case, 13 out of 20 observed areas had at least one cell showing only mCherry. Western blotting showed equivalent levels of ORF3:Myc and ORF4:Myc expression (Fig. 2e). Taken together, these results suggest that CMoV ORF4 protein can target PD, induce the formation of tubules and increase the size exclusion limit of PD.

### ORF4 protein facilitates the cell-to-cell movement of a CMoV replicon

To explore whether the ORF4 protein is directly involved in virus movement, we attempted to insert the GFP coding sequence at multiple sites of the CMoV infectious clone backbone, the expression of which would enable us to trace the virus movement. Unfortunately, those attempts were not successful (data not shown). As an alternative approach, we engineered the replicon CMoV ORF1/2:GFP (Fig. 1) by substituting the overlapping sequences of ORF3/4 protein coding region with the coding sequence of GFP, while the vRdRp coding sequences (ORF1/2) were maintained. Similar replicons have been established for many animal viruses, and

proved to be valuable tools for the study of virus infection (Kato *et al.*, 2003; Kato & Hishiki, 2016).

First, we validated that CMoV ORF1/2:GFP is truly a replicon. *Nicotiana benthamiana* leaves were agroinfiltrated with the *A. tumefaciens* harboring the construct pJL89//CMoV ORF1/2:GFP. At 10 d post-agroinfiltration, the GFP expression was confirmed by microscopy imaging and Western blotting (data not shown). The total RNAs were extracted and subjected to Northern blotting. As shown in Fig. 3(a), the infection of CMoV ORF1/2:GFP produced a significant amount of *gfp* RNA transcripts in the form of viral subgenomic RNA (sgRNA). These data show that the CMoV ORF1/2:GFP is capable of replicating on its own.

Then, we tested whether the ORF3 or ORF4 protein has an impact on the vRNA accumulation/replication in cells. Protoplasts were isolated from *N. benthamiana* leaves, and were transfected with an equal amount of plasmid pJL89//CMoV ORF1/2:GFP, together with plasmid pART27/ORF3:Myc, pART27/ORF4:Myc or both plasmids. The presence of the ORF3 and/or ORF4 proteins did not affect the vRNA accumulation (Fig. 3b,

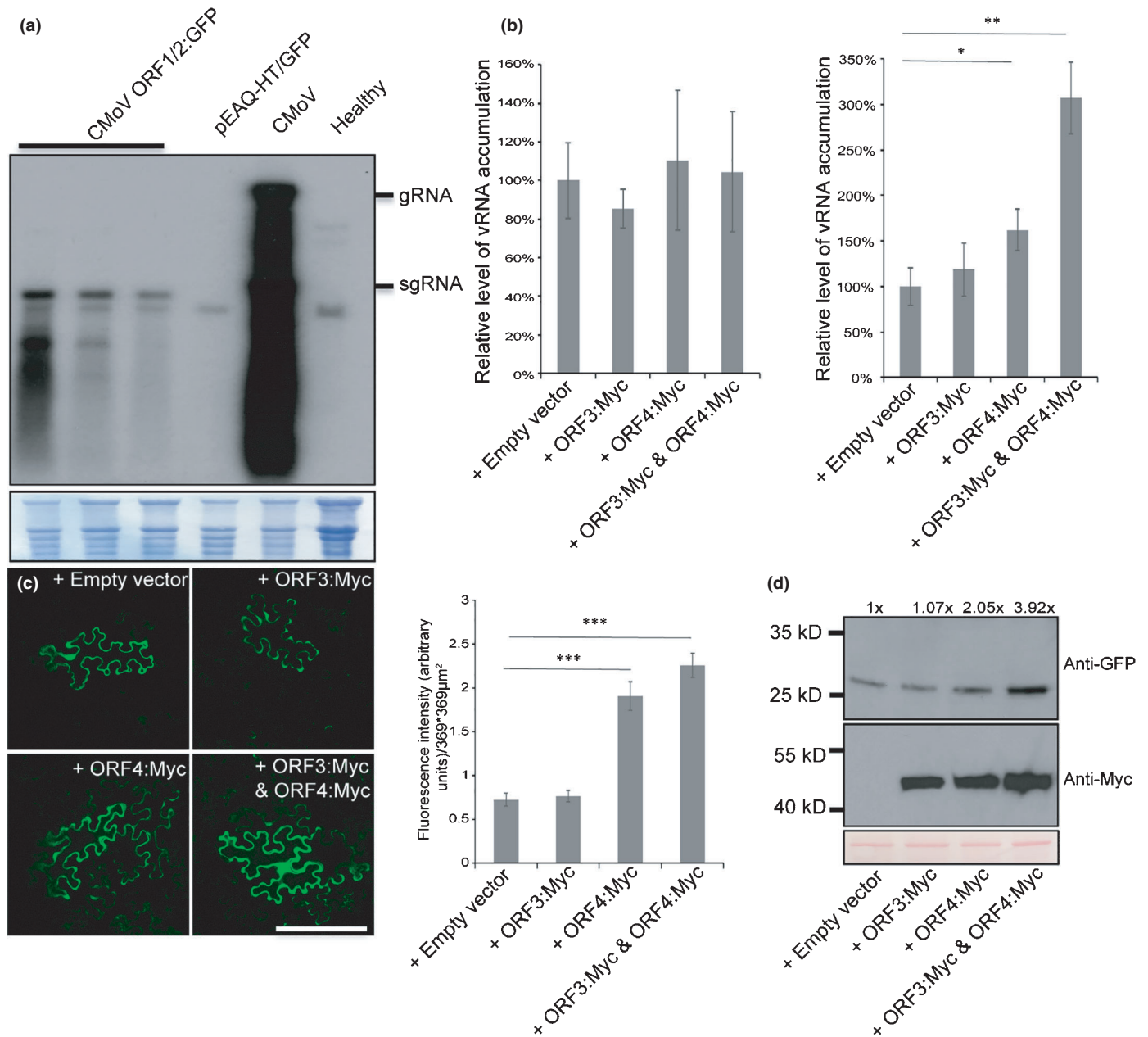


**Fig. 3** Quantification of viral RNA (vRNA) accumulation in the presence of the ORF3 and ORF4 proteins. (a) *Nicotiana benthamiana* leaves were agroinfiltrated with pJL89//CMoV ORF1/2:GFP, pEAQ-HT/GFP and pJL89/CMoV. The total RNAs were then extracted at 10 d post-agroinfiltration and subjected to Northern blotting. The methylene blue-stained membrane is shown in the lower panel, indicating equal loading of the RNA samples. The Northern blotting was done with probes bind to the 3' untranslated region (3' UTR) of the *Carrot mottle virus* (CMoV) genomic RNA. (b) *Nicotiana benthamiana* protoplasts (b, left panel) or the leaf tissues (b, right panel) were infected with CMoV ORF1/2:GFP, together with the expression of empty vector, ORF3:MyC, ORF4:MyC, and both ORF3:MyC and ORF4:MyC. The vRNA accumulation levels were then quantified by quantitative reverse transcription polymerase chain reaction. The agroinfiltrated leaves were observed by confocal microscopy. The representative images of the infection foci are shown in (c) (left panel). The average fluorescence intensity of the infection foci ( $n = 20$ ) was quantified with IMAGEJ (c, right panel). Significant difference is indicated by asterisks (Student's  $t$ -tests: \*\*\*,  $P < 0.001$ ; \*\*,  $0.001 < P < 0.01$ ; \*,  $0.01 < P < 0.05$ ). Mean values  $\pm$  SD from three independent experiments are shown (b, c). The leaf tissues were further processed, and the protein expression levels were checked by Western blotting (d). The green fluorescent protein (GFP) band intensity was quantified with IMAGEJ, and the relative values were shown on top of the blot (d). The Ponceau S stained Ribulose large subunit serves as a loading control. The Western blotting was done with anti-GFP and anti-MyC antibodies.

left panel). We then performed the same experiment, but in the agroinfiltrated *N. benthamiana* leaves. The ORF4 protein, alone or in combination with the ORF3 protein, enhanced the vRNA accumulation in the leaf tissues when quantified by quantitative

reverse transcription polymerase chain reaction (RT-qPCR) (Fig. 3b, right panel). The leaf tissues were further observed by confocal microscopy. We found that the majority of infection foci were only one GFP-fluorescent cell in the presence of empty

vector or the ORF3 protein, while multiple fluorescent cells were found when the ORF4 protein was expressed alone or with the ORF3 protein (Fig. 3c). The average fluorescence intensity of the infection foci was further quantified. Consistently, the fluorescence intensity was much higher in the presence of ORF4 protein, with or without the ORF3 protein (Fig. 3c, right panel). The GFP accumulation was further confirmed by Western blotting (Fig. 3d). These data suggest that the ORF4 protein facilitates the virus cell-to-cell movement of CMoV.

### A lysine residue and two potential SUMO-interacting motifs (SIMs) are required for efficient ORF4 protein PD targeting

SUMOylation and SUMO interactions have been shown to alter protein localization, and further affect their biological functions (Gareau & Lima, 2010). Our preliminary bioinformatic analysis showed the presence of potential SUMOylation site(s) in the ORF4 protein. How the host cell SUMOylation pathway can be hijacked by the viral pathogens, in particular, plant viruses, is still largely unknown. To explore if SUMOylation or SUMO interaction plays a role in ORF4 protein PD targeting, potential critical amino acid residues were characterized. The ORF4 protein has six lysine residues that could be SUMO conjugation sites, although none of them exist within a consensus context. These lysine residues, at positions 5, 68, 69, 78, 115 and 240 were substituted with alanine, giving mutants ORF4<sup>K5A</sup>:GFP, ORF4<sup>K68A-K69A</sup>:GFP, ORF4<sup>K78A</sup>:GFP, ORF4<sup>K115A</sup>:GFP and ORF4<sup>K240A</sup>:GFP. We also predicted potential SIMs using the online servers GPS-SUMO (<http://sumosp.biocuckoo.org/index.php>) (Zhao *et al.*, 2014) and JASSA (<http://www.jassa.fr/?m=jassa>) (Beauclair *et al.*, 2015). SIMs are generally characterized by a short stretch of hydrophobic amino acids, which are flanked by acidic amino acid residues (Gareau & Lima, 2010). Three candidate SIMs with the highest scores, LINLL (SIM1), LVIVF (SIM2) and VIWV (SIM3), were changed to alanine. The resulting mutants are ORF4<sup>LINLL-AAAAA</sup>:GFP, ORF4<sup>LVIVF-AAAAA</sup>:GFP and ORF4<sup>VIWV-AAAAA</sup>:GFP, and are hereafter designated as ORF4<sup>SIM1 Mut</sup>:GFP, ORF4<sup>SIM2 Mut</sup>:GFP and ORF4<sup>SIM3 Mut</sup>:GFP.

*Nicotiana benthamiana* leaves were separately agroinfiltrated with WT and the mutated ORF4 protein GFP fusion constructs, and the cellular locations of these protein fusions were observed using confocal microscopy. Similar to the WT ORF4:GFP, the mutants ORF4<sup>K5A</sup>:GFP, ORF4<sup>K68A-K69A</sup>:GFP, ORF4<sup>K115A</sup>:GFP and ORF4<sup>K240A</sup>:GFP still accumulated at PD (Fig. 4a). Mutant ORF4<sup>K78A</sup>:GFP also targeted to PD; however, the size of the PD-localized structures was much smaller. The fluorescence intensity of PD/PM was further quantified. The value was  $4.19 \pm 0.25$  ( $n=60$ ) for the WT ORF4:GFP protein, while it decreased to  $1.87 \pm 0.21$  ( $n=60$ ) for the mutated ORF4<sup>K78A</sup>:GFP protein. For mutants in which the potential SIMs were replaced, mutant ORF4<sup>SIM1 Mut</sup>:GFP was similar to the WT ORF4:GFP. However, mutants ORF4<sup>SIM2 Mut</sup>:GFP and ORF4<sup>SIM3 Mut</sup>:GFP failed to target the PD efficiently (Fig. 4a). The protoplasts were then isolated from the leaves expressing the

WT and mutated ORF4:GFP proteins and were examined by confocal microscopy. The mutation of the K78, SIM2 and SIM3 abolished the formation of the ORF4 protein-induced tubules (Fig. 4b). We also isolated the CW fraction and, when examined by Western blot analysis, we found that the ORF4<sup>SIM2 Mut</sup>:GFP and ORF4<sup>SIM3 Mut</sup>:GFP were still CW-associated (Fig. 4c; see also the Discussion section). Western blotting showed equivalent abundances of proteins for the ORF4 mutants, except for mutant ORF4<sup>K78A</sup>:GFP, for which the protein accumulation level was reduced (Fig. 4d). These results suggest that the residue K78 and the two potential SIMs (SIM2 and SIM3) of the ORF4 protein are required for its PD efficient targeting.

As shown earlier, the ORF4 protein can modify and increase the size exclusion limit of PD. To further assess whether residue K78, SIM2 and SIM3 are important for this function of the ORF4 protein, we coexpressed the mutated ORF4 proteins with the reporter HDEL:GFP//dmCherry. *Nicotiana benthamiana* leaves were agroinfiltrated with the empty vector, ORF4:Myc, ORF4<sup>K78A</sup>:Myc, ORF4<sup>SIM1 Mut</sup>:Myc, ORF4<sup>SIM2 Mut</sup>:Myc, ORF4<sup>SIM3 Mut</sup>:Myc, together with the reporter HDEL:GFP//dmCherry. Similar to with the WT ORF4 protein, the dmCherry protein was still able to move to the neighboring cells in the presence of mutated protein ORF4<sup>K78A</sup>:Myc and ORF4<sup>SIM1 Mut</sup>:Myc (Fig. 4e). As expected, no cells showing dmCherry alone were found in the neighboring cells when ORF4<sup>SIM2 Mut</sup>:Myc and ORF4<sup>SIM3 Mut</sup>:Myc were present. Protein expression of all the Myc-tagged ORF4 proteins was confirmed by Western blotting (Fig. 4f). These data suggest, in particular, that the two potential SIMs are important for the ORF4 PD targeting as well as its ability to increase the size exclusion limit of PD.

### ORF4 protein interacts with host SUMOylation factor SCE1, SUMO1 and SUMO2, leading to its SUMOylation

We then tested if the ORF4 protein can interact with host cell SUMOylation factors using bimolecular fluorescence complementation (BiFC). In order to maintain the functionality of the ORF4 protein, we made constructs that fused either the N-terminal half of GFP (ntGFP) or the C-terminal half of GFP (ctGFP) to the C-terminus of the ORF4 protein. The resulting fusions were designated as ORF4:ntGFP and ORF4:ctGFP. First, we tested the fluorescence complementation of two different combinations: ORF4:ntGFP and ctGFP, ORF4:ctGFP and ntGFP. The cells expressing ORF4:ntGFP and ctGFP showed no fluorescence, while the expression of ORF4:ctGFP and ntGFP showed weak fluorescence (Fig. 5a). Consequently, for the following BiFC assay, the construct ORF4:ntGFP was used. In the model plant *A. thaliana*, only four of the SUMO proteins (SUMO1, 2, 3 and 5) are known to be functional (Saracco *et al.*, 2007; Budhiraja *et al.*, 2009). Therefore, the coding sequences of SUMO1, 2, 3, 5 as well as SCE1 were amplified from *A. thaliana* (Col-0). As the C-terminus of SUMOs will be processed to expose the Gly-Gly motif, constructs were made to fuse the SUMOs and SCE1 to the C-terminus of ctGFP. *Nicotiana benthamiana* cells expressing ORF4:ntGFP, together with ctGFP:SCE1, ctGFP:SUMO1



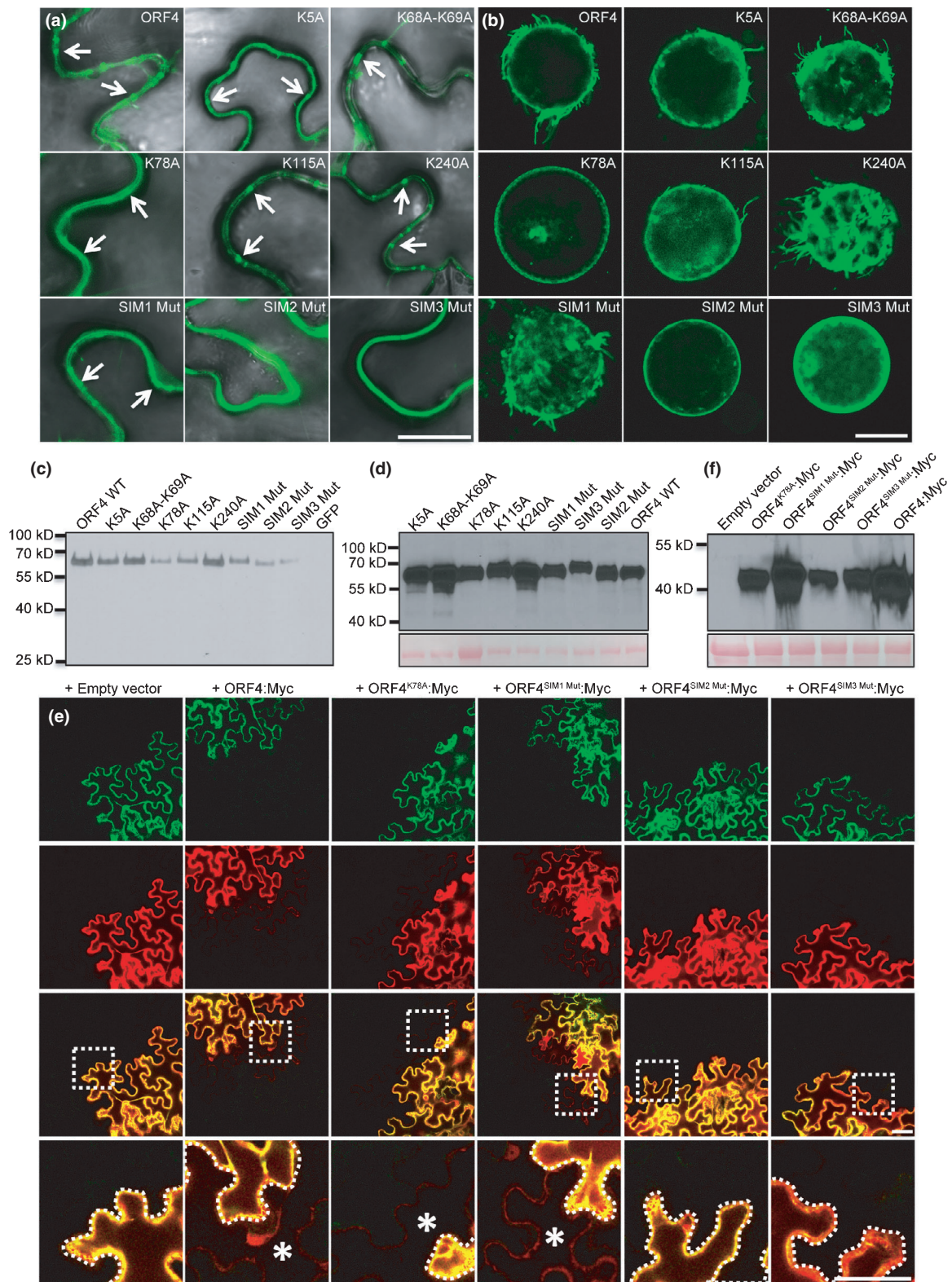


**Fig. 4** Characterization of ORF4 amino acid residues that are important for targeting plasmodesmata (PD). (a) *Nicotiana benthamiana* leaf tissues expressing the WT and the mutated ORF4:GFP fusion proteins at 72 h after agroinfiltration. The protoplasts were isolated from the above leaf tissues, and were observed by confocal microscopy 40 h later (b). The cell wall fractions (c) and the total proteins (d) were extracted from the above leaf tissues and processed for Western blot with anti-GFP antibodies. (e) Confocal microscopy imaging of the *N. benthamiana* leaf tissues expressing empty vector, WT and mutated ORF4:Myc, together with the reporter HDEL:GFP//dmCherry. (f) The leaf tissues were processed for Western blot with anti-Myc antibodies. The Ponceau S stained Rubisco large subunit serves as a loading control (d, f). The areas outlined by the white boxes are enlarged in the lowest panels (e). The arrows in (a) indicate the PD, and the stars in (e) highlight the cell showing mCherry only. Bars: (a, b) 20  $\mu$ m; (e) 50  $\mu$ m.



and ctGFP:SUMO2, showed bright fluorescence (Fig. 5a, left panels). Furthermore, we found the fluorescent signals at the nucleus and PD (Fig. 5a, right panels). By contrast, cells expressing ORF4:ntGFP with ctGFP:SUMO3 and ctGFP:SUMO5 showed no fluorescence complementation, although fluorescent aggregates were visualized occasionally (Fig. 5a, left panels). To further confirm the interaction of the ORF4 protein with host cell SUMOylation factors, we performed coimmunoprecipitation (co-IP) experiments. Protein GFP, SCE1:GFP, GFP:SUMO1, GFP:SUMO2, GFP:SUMO3 and GFP:SUMO5 were transiently expressed with ORF4:Myc in *N. benthamiana* leaves, and the interaction was assayed by coimmunoprecipitation of the GFP fusion proteins. As shown in Fig. 5(d), the negative control did not show any coprecipitation, indicating that ORF4:Myc did not bind to the GFP-Trap beads. However, the ORF4:Myc fusion protein did coimmunoprecipitate with SCE1:GFP, GFP:SUMO1 and GFP:SUMO2 (Fig. 5d). No coimmunoprecipitation of the ORF4:Myc fusion protein was found with host cell SUMO3 and SUMO5 proteins (Fig. 5d). These results suggest that the ORF4 protein interacts with the host cell SCE1, SUMO1 and SUMO2, but not with SUMO3 and SUMO5 proteins.

Next, we investigated if the ORF4-SCE1, ORF4-SUMO1 and ORF4-SUMO2 interactions were mediated by the above characterized ORF4 protein K78, SIM2 and/or SIM3. The ORF4 mutants (ORF4<sup>K78A</sup>, ORF4<sup>SIM1 Mut</sup>, ORF4<sup>SIM2 Mut</sup> and ORF4<sup>SIM3 Mut</sup>) were fused to the N-terminus of ntGFP. These mutants and WT ORF4:ntGFP were then coexpressed with ctGFP:SCE1, ctGFP:SUMO1 and ctGFP:SUMO2. As shown in Fig. 5(b), compared with the WT ORF4 protein, the fluorescence intensity was much lower when the SIM2 and SIM3 were replaced (Fig. 5b). Statistically, the fluorescence intensities were significantly reduced by *c.* 80% and 50%, for the interaction of ORF4<sup>SIM2 Mut</sup> or ORF4<sup>SIM3 Mut</sup> with SCE1, SUMO1 and SUMO2, respectively (Fig. 5c). We then confirmed the weaker interaction of mutant ORF4<sup>SIM2 Mut</sup> and ORF4<sup>SIM3 Mut</sup> with SCE1 by co-IP. Consistently, ORF4<sup>SIM2 Mut</sup> and ORF4<sup>SIM3 Mut</sup> coimmunoprecipitated with host protein SCE1, but to a much lower extent (Fig. 5e).

To demonstrate whether the interaction with SCE1, SUMO1 and SUMO2 leads to the SUMOylation of the ORF4 protein, we performed *E. coli in vivo* SUMOylation assays. As has been mentioned by others (Sánchez-Durán *et al.*, 2011; Xiong & Wang, 2013), protein SUMOylation is challenging to confirm *in planta* as a result of the presence of a fast and efficient deSUMOylation pathway. Thus, we felt that the *E. coli in vivo* SUMOylation assay was our best choice. The *A. thaliana* transcription factor AtMYB30, a known SUMO target protein (Colby *et al.*, 2006; Okada *et al.*, 2009), was chosen as positive control for the assay. As the C-terminal Gly-Gly motif is important for the SUMO attachment, the mutation of Gly-Gly to Ala-Ala motif will make the SUMO nonfunctional, and thus it was used as negative control for the assay (Okada *et al.*, 2009). The amino acid sequences of AtSUMO1 and AtSUMO2 are almost identical (Fig. 7a), and thus only AtSUMO1 was selected for this assay. As shown in Fig. 5(f), the positive control AtMYB30 was

SUMOylated in the presence of functional SUMO1(GG), while this was not the case in the presence of nonfunctional SUMO1 (AA). Similarly, we found that the protein ORF4 was SUMOylated. The mutation of K78, SIM2 and SIM3 affected the protein SUMOylation dramatically (Fig. 5f). Altogether, these results show that the ORF4 protein interacts with host cell SUMOylation factors, SCE1, SUMO1 and SUMO2, and motifs, K78, SIM2 and SIM3 are involved in this interaction, further leading to the SUMOylation of this protein.

### K78, SIM2 and SIM3 are required for efficient virus movement

To see if K78, SIM2 and/or SIM3 are important for CMoV virus infection in plants, the mutations ORF4<sup>K78A</sup>, ORF4<sup>SIM2 Mut</sup> and ORF4<sup>SIM3 Mut</sup> were introduced into a CMoV infectious clone (pJL89/CMoV = WT CMoV). As CMoV ORF3 and ORF4 overlap almost completely, the introduction of mutations ORF4<sup>K78A</sup>, ORF4<sup>SIM2 Mut</sup> and ORF4<sup>SIM3 Mut</sup> also introduced mutations into the ORF3 protein. These resulted in ORF3<sup>E85G</sup>, ORF3<sup>A86G-R87S-H88C-V90S-R91C</sup> and ORF3<sup>D104G-L105C</sup>, respectively. These mutated ORF3:GFP fusion proteins were expressed in *N. benthamiana* leaves transiently, and their subcellular distributions were the same as for the WT ORF3:GFP fusion (see Fig. S1). The *N. benthamiana* leaves were agroinfiltrated with the clones expressing CMoV<sup>K78A</sup>, CMoV<sup>SIM2 Mut</sup>, CMoV<sup>SIM3 Mut</sup> and WT CMoV. Total RNAs were extracted at 5 d post-agroinfiltration, and an equal amount of RNA was used for Northern blotting. In all cases, the viral genomic RNA (gRNA) and sgRNA could be detected, although at reduced levels for the mutants (Fig. 6a). The *N. benthamiana* protoplasts were transfected with these infectious clones, and the levels of vRNA accumulation were quantified by RT-qPCR. Although the K78A mutation showed reduced vRNA accumulation by 30%, the mutations of SIM2 and SIM3 did not affect the vRNA accumulation (Fig. 6b, left panel). These data show that the mutated viruses are still replication-competent, and the vRNA accumulation levels are similar to those of the WT virus.

We then quantified the vRNA accumulation in the WT and mutated virus clone agroinfiltrated *N. benthamiana* leaves. Compared with the protoplast assay, the leaf assay allows us to see if these motifs are important for the virus cell-to-cell movement. The vRNA levels were similar for CMoV<sup>K78A</sup>, CMoV<sup>SIM2 Mut</sup> and CMoV<sup>SIM3 Mut</sup>, but these were reduced to 3% of WT CMoV vRNA levels (Fig. 6b, right panel). This result suggests that the mutations of K78, SIM2 and SIM3 affected the virus cell-to-cell movement significantly. The CMoV infection was also assessed in the upper nonagroinfiltrated leaves by RT-PCR. At 2 wk post-agroinfiltration (wpa), CMoV was detected in all three plants agroinfiltrated with WT CMoV (Fig. 6c, upper panel). Only one out of three CMoV<sup>K78A</sup>-infected plants developed a systemic infection, and none of the CMoV<sup>SIM2 Mut</sup>- and CMoV<sup>SIM3 Mut</sup>-infected plants were systemically infected (Fig. 6c, upper panel). At 3 wpa, all three CMoV<sup>K78A</sup>-infected plants were systemically infected (Fig. 6c, lower panel). However, still none of the

CMoV<sup>SIM2 Mut</sup>- and CMoV<sup>SIM3 Mut</sup>-infected plants developed systemic infections. To exclude the possibility that CMoV<sup>K78A</sup> turned out to be a revertant, the *ORF4* fragment was amplified from the systemically infected leaf tissues. DNA sequencing

showed the mutations were retained (Fig. 6d). Taken together, these data demonstrate that mutations affecting K78, SIM2 and SIM3 affected efficient CMoV cell-to-cell and systemic movement.

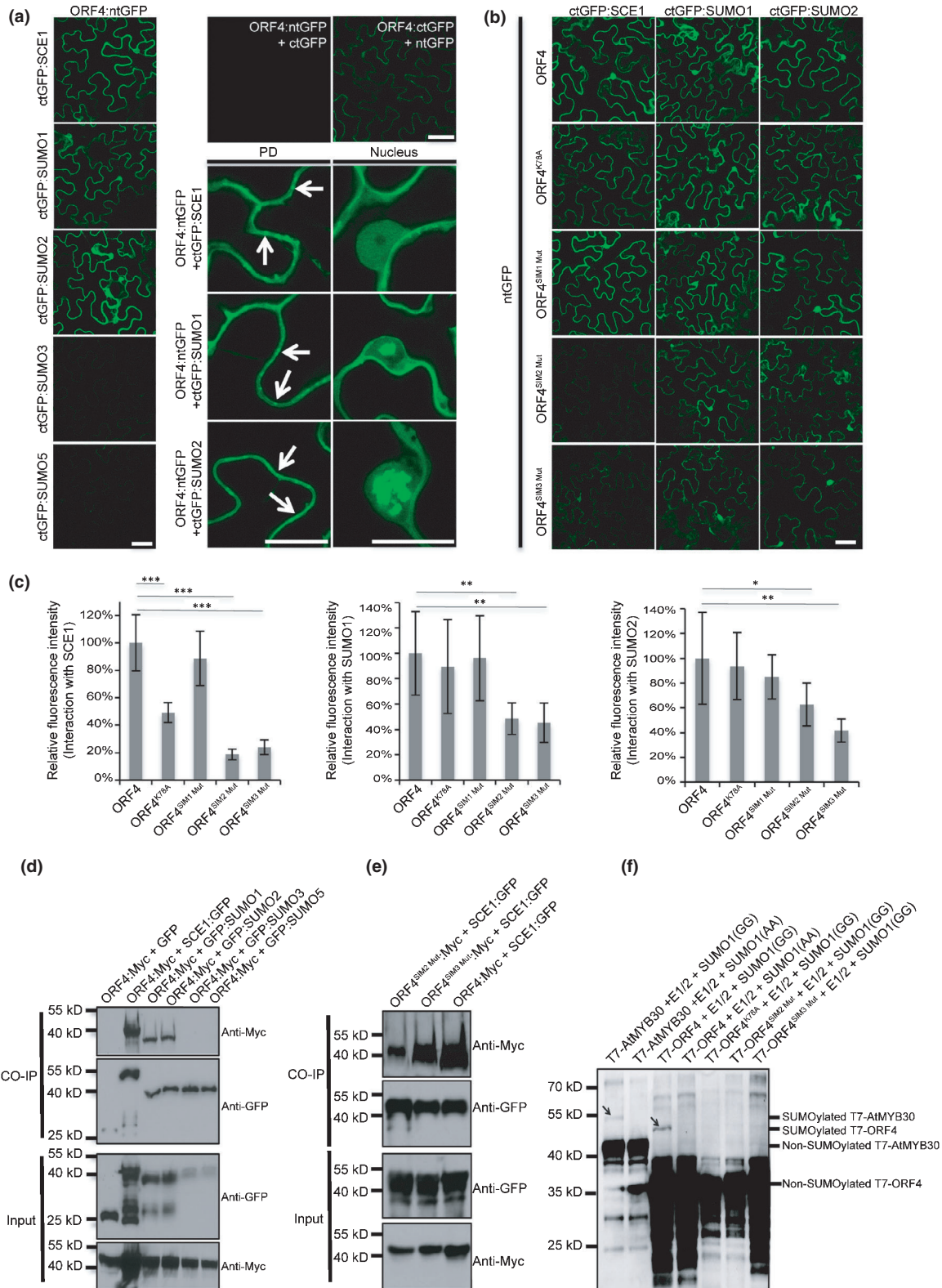


**Fig. 5** Bimolecular fluorescence complementation and coimmunoprecipitation assays of ORF4 protein and SCE1, small ubiquitin-like modifier (SUMO) interactions. Bimolecular fluorescence complementation assay for protein–protein interactions between the wild-type (WT) ORF4 protein (a) and the mutated ORF4 proteins (b) with the host proteins SCE1, SUMO1 and SUMO2. *Nicotiana benthamiana* leaf tissues expressing different N-terminal half of GFP (ntGFP) and C-terminal half of GFP (ctGFP) combinations were checked at 48 h after agroinfiltration. The arrows in (a) point at the plasmodesmata (PD). Bars: (a, lower right panels) 20  $\mu\text{m}$ ; (a (left and upper right panels), b) 50  $\mu\text{m}$ . (c) Statistical analysis of the bimolecular fluorescence complementation fluorescence intensity of the ORF4 proteins with the host protein SCE1, SUMO1 and SUMO2. The average fluorescence intensity was quantified with IMAGEJ, and the sample number ( $n$ ) is 25 for each tested combination. Significant difference is indicated by asterisks (Student's  $t$ -tests: \*\*\*,  $P < 0.001$ ; \*\*,  $0.001 < P < 0.01$ ; \*,  $0.01 < P < 0.05$ ). Mean values  $\pm$  SDs of three independent experiments are shown. (d, e) Coimmunoprecipitation detects the interaction among the WT, mutated ORF4 proteins and the host protein SCE1 and SUMOs. (f) *Escherichia coli* cells transformed with different combinations of the three plasmids that encode the proteins are indicated above each lane. The positive control T7-AtMYB30 (lane 1 and 2) was encoded by the plasmid pET28a(+)-AtMYB30, and the WT (lane 3 and 4) or mutated (lane 5, 6 and 7) T7-ORF4 proteins were encoded by the corresponding pET28a(+)-ORF4 constructs. Protein E1 (all lanes) was encoded by the plasmid pACYC/SAE2-SAE1b. Protein E2 + SUMO1(GG) (lanes 1, 3, 5, 6 and 7) was encoded by the plasmid pCDF/SUMO1(GG)-SCE1a. Protein E2 + SUMO1(AA) (lanes 2 and 4) was encoded by the plasmid pCDF/SUMO1(AA)-SCE1a. The SUMO1(GG) is functional, while the SUMO1(AA) is nonfunctional and can be used as the negative controls. SUMOylated AtMYB30 (lane 1 vs 2) and ORF4 protein (lane 3 vs 4) were observed as bands shifted to higher molecular weight, and the bands are highlighted with arrows. The Western blot was performed with anti-T7 tag antibodies.

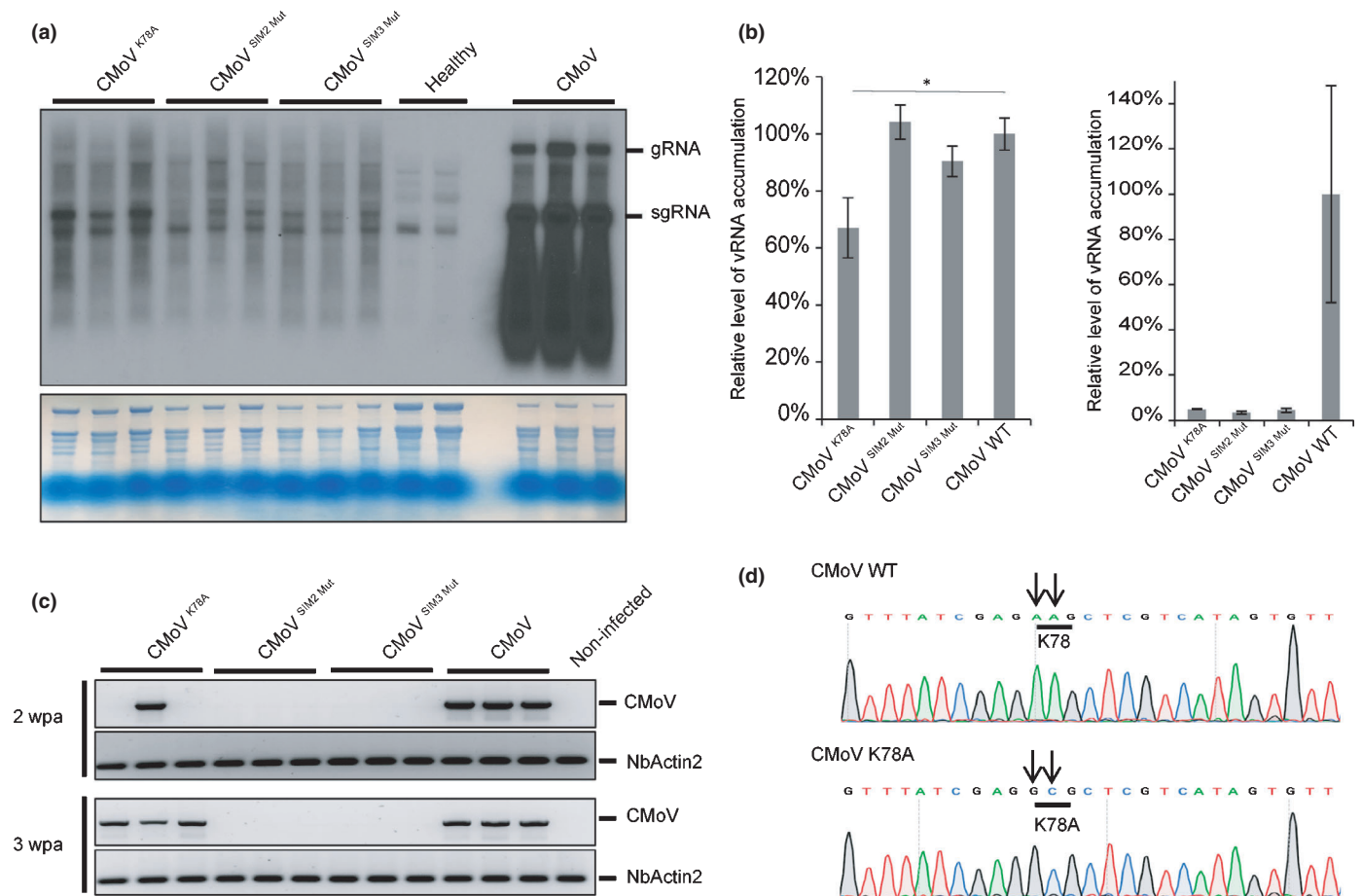


**Fig. 6** The critical motifs are required for efficient *Carrot mottle virus* (CMoV) infection. (a) *Nicotiana benthamiana* plants were agroinfiltrated with wild-type and mutated CMoV constructs, and the viral RNA (vRNA) accumulation was detected by Northern blotting. *Nicotiana benthamiana* protoplasts were transfected with these constructs (b, left panel) or the agroinfiltrated leaf tissues (b, right panel) were processed, and the level of vRNA accumulation was quantified by quantitative reverse transcription polymerase chain reaction. The methylene blue-stained membrane is shown in the lower panel, indicating equal loading of the RNA samples (a). Significant difference is indicated by asterisks (Student's  $t$ -tests: \*,  $0.01 < P < 0.05$ ). Mean values  $\pm$  SDs of three independent experiments are shown (b). vRNA accumulation in the upper nonagroinfiltrated leaves detected by reverse transcription polymerase chain reaction at 2 and 3 wk after agroinfiltration (wpa) (c). The *NbActin2* is used as the internal control (b, c). (d) DNA sequencing chromatogram of wild-type and mutated ORF4 fragment (partial). The upper arrows indicate the original nucleotides in the viral genome, and the lower arrows indicate the changed nucleotides that were introduced during mutagenesis.





## Host protein SCE1 and SUMO are required for efficient virus infection

To investigate whether host proteins SCE1 and SUMO are important for CMoV infection, we sought to assess CMoV infection using available *A. thaliana* knockouts. However, we found that *A. thaliana* is not susceptible to CMoV infection, either by agroinfiltration or by rub inoculation (see Fig. S2). We then took an alternative approach of knocking down the mRNA levels of *NbSCE1* and *NbSUMO* using a TRV-based virus-induced gene silencing system, and then measured the CMoV vRNA accumulation in the susceptible host *N. benthamiana* by RT-qPCR. First, we compared the amino acid sequences of *NbSCE1* vs *AtSCE1* and *NbSUMO* vs *AtSUMO1/2* (Fig. 7a). The identity was 88.1% between *NbSCE1* and *AtSCE1*, and 94.4% between *NbSUMO* and *AtSUMO1* (96.6% with *AtSUMO2*). We also confirmed that *NbSCE1* and *NbSUMO* can interact with the CMoV ORF4 protein *in planta* (Fig. 7b). This suggests that the function of *NbSCE1* and *NbSUMO* is similar to their *A. thaliana* paralogs.

We then cloned sequences of *NbSCE1* and *NbSUMO* into TRV:RNA2, in both the sense and anti-sense orientations. *Nicotiana benthamiana* plants were agroinfiltrated with the TRV:RNA2, TRV:RNA2-*NbSCE1* sense, TRV:RNA2-*NbSCE1* anti-sense, TRV:RNA2-*NbSUMO* sense, TRV:RNA2-*NbSUMO* anti-sense, together with TRV:RNA1. *Nicotiana benthamiana* plants agroinfiltrated with TRV:RNA2-*NbPDS* and TRV:RNA1 were used as controls (Bachan & Dinesh-Kumar, 2012). The upper newly emerged leaves were evaluated to quantify the silencing efficiency of *NbSCE1* and *NbSUMO* by RT-qPCR at 1 wk post-agroinfiltration. As shown in Fig. 7(c), up to 70–80% of *NbSCE1* and *NbSUMO* mRNAs were silenced. The upper young leaves were then agroinfiltrated with the CMoV infectious clone, and the CMoV vRNA accumulation was quantified at 1 wk post-agroinfiltration. Compared with the TRV control, the vRNA level was reduced 50–80% and 70–80% in the *NbSCE1*- and *NbSUMO*-silenced plants, respectively (Fig. 7d). These results suggest that host proteins SCE1, SUMO1 and SUMO2 play important roles in CMoV infection.

## The SIM2 motif is highly conserved among different umbraviruses

To expand our findings and assess whether similar amino acid signatures may be found in the ORF4 proteins encoded by other umbraviruses, we aligned the ORF4 protein amino acid sequences of different umbraviruses. The alignment was done using the online server CLUSTAL OMEGA (<https://www.ebi.ac.uk/Tools/msa/clustalo/>). None of the lysine residues, except K78, are conserved (Fig. 8a). The SIM1 and SIM2, but not SIM3, are highly conserved among *Umbravirus* ORF4 proteins. As we showed earlier, the SIM1 did not affect ORF4 protein PD targeting. Consequently, to test the importance of these conserved residues for PD targeting, mutations replacing the K78 and SIM2 were introduced into the P27 protein of PEMV2. The resulting mutated protein fusions were designated P27<sup>K78A</sup>:GFP

and P27<sup>VVVVF-AAAAA</sup>:GFP. *Nicotiana benthamiana* leaf tissues expressing the mutated protein fusions were observed by confocal microscopy. Similar to WT P27:GFP (Fig. 8b, left panel), P27<sup>K78A</sup>:GFP still could target PD (Fig. 8b, middle panel). However, the mutant P27<sup>VVVVF-AAAAA</sup>:GFP could not target PD (Fig. 8b, right panel). These data indicate (at least in the case of PEMV2) that, as for the CMoV ORF4 protein, the SIM2 of PEMV2 P27 is important for its PD targeting.

## Discussion

Plant virus MPs play critical roles in regulating the spread of virus infections in plants. Thus, understanding how MPs target to and regulate PD is of great importance. This information could be used in fundamental cell biology but is also potentially important for the development of virus-resistant crop plants. In this work, we showed that both N-terminal and C-terminal GFP-fused CMoV ORF4 protein can target PD (Fig. 2a,b). This indicates the ORF4 protein harbors a signal that can direct its PD localization. However, the size of GFP:ORF4-induced punctae remained quite constant, whereas the size of ORF4:GFP-induced tubules that traverse the PD increased over the 72 h period (Fig. 2a). The formation of tubules by the ORF4 protein was confirmed in protoplasts (Fig. 2a). This is consistent with what has been shown for another *Umbravirus*, GRV, of which the ORF4 protein induces tubule formation in protoplasts (Ryabov *et al.*, 1998). Many other plant viruses, such as *Grapevine fanleaf virus*, *Alfalfa mosaic virus* and CPMV, can also induce the formation of tubules for virus movement (Wellink *et al.*, 1993; Kasteel *et al.*, 1997; Laporte *et al.*, 2003). It has been suggested that their virions move through the tubules for the virus cell-to-cell movement. Different from these other plant viruses, umbraviruses do not encode a capsid protein and in single infections have no virions; thus it will be interesting to visualize the cell-to-cell movement of the CMoV RNPs through the modified PD. It has been shown that, in the case of GRV, the ORF3 protein mediates virus long-distance movement and the ORF4 protein facilitates virus cell-to-cell movement. This was done by introducing the ORF3 and ORF4 viral proteins into a heterologous virus (Ryabov *et al.*, 1999b; Kim *et al.*, 2007b). Direct evidence elucidating the functions of the ORF3 and ORF4 proteins for native *Umbravirus* movement, and how these two proteins work together for the virus movement, was still missing.

In this work, our efforts, which aimed to make fluorescent protein-tagged CMoV infectious clone to trace the virus cell-to-cell movement, were unsuccessful (data not shown). Instead, we constructed a dual fluorescent protein reporter HDEL:GFP//dmCherry (Fig. 1). When coexpressed with the ORF3 and ORF4 viral proteins, we found that the ORF4 protein, but not the ORF3 protein, supported the cell-to-cell movement of dmCherry (Fig. 2d). To further explore the role of the ORF4 protein in virus infection, to the best of our knowledge, we have established the first replicon for an *Umbravirus*. Using this replicon as a reporter, we have shown that the ORF4 protein can facilitate the cell-to-cell movement of CMoV (Fig. 3). Furthermore, we introduced the mutations (ORF4<sup>K78A</sup>, ORF4<sup>SIM2 Mut</sup> and ORF4<sup>SIM3</sup>

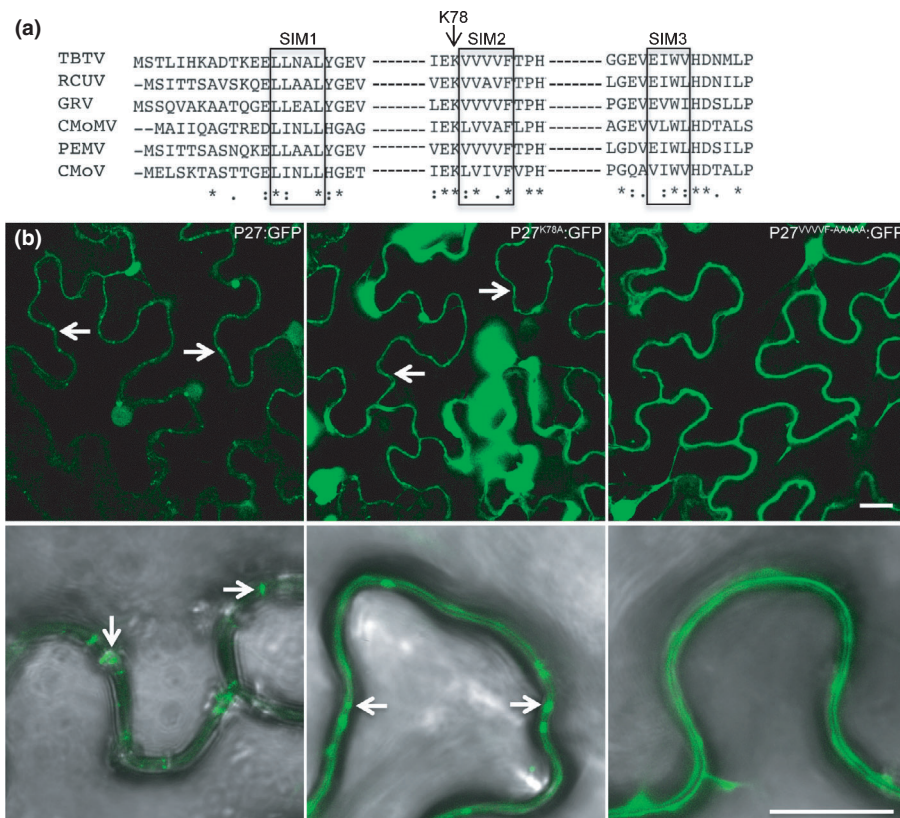


**Fig. 8** SIM2 is conserved among *Umbravirus* movement proteins. (a) Alignment of part of the *Umbravirus* movement proteins. TBTv, *Tobacco bushy top virus*; RCUV, *Red clover umbravirus*; GRV, *Groundnut rosette virus*; CMoMV, *Carrot mottle mimic virus*; PEMV, *Pea enation mosaic virus-2*; CMoV, *Carrot mottle virus*. Identical amino acid residues that are highly conserved are highlighted by stars, and similar amino acid residues are indicated by dots. The arrow indicates the lysine residue at position 78, and the SIMs are highlighted by the box. (b) *Nicotiana benthamiana* cells expressing P27:GFP, as well as its mutated protein P27<sup>K78A</sup>:GFP and P27<sup>VVVVF-AAAAA</sup>:GFP. The green fluorescent protein (GFP) channels are shown on the top, and the lower panels are the GFP and bright field merged channels. The arrows indicate the plasmodesmata (PD). Bars, 20  $\mu$ m.

<sup>Mut</sup>) that affected PD targeting of the ORF4 protein into the CMoV infectious clone. The mutation ORF4<sup>K78A</sup> led to less efficient PD targeting of the ORF4 protein (Fig. 4a), thus slowing the CMoV systemic infection (Fig. 6c). The mutations ORF4<sup>SIM2 Mut</sup> and ORF4<sup>SIM3 Mut</sup>, both of which dramatically prevented the ORF4 protein from localizing to the PD (Fig. 4a), completely abolished CMoV systemic infection (Fig. 6c). These results suggest that the PD targeting of the ORF4 protein is positively correlated with the virus movement. We confirmed that these CMoV mutants could still accumulate to similar levels in protoplasts (Fig. 6b). This excludes the possibility that the mutations impaired virus replication. Based on these data, we conclude that the ORF4 protein is a primary determinant for the cell-to-cell movement of CMoV. Additionally, the ORF4 protein-dependent cell-to-cell movement was enhanced in the presence of the ORF3 protein (Fig. 3). For another *Umbravirus*, GRV, the ORF3 protein can bind the vRNA (Taliensky *et al.*, 2003). Consequently, we propose a TGBs-like working model: the CMoV ORF3 binds the vRNA to form vRNPs, and the vRNPs can be relocalized to the PD for the virus movement through the ORF3–ORF4 protein interaction.

We found that the ORF4 protein selectively interacts with the *A. thaliana* proteins SCE1, SUMO1 and SUMO2, but not

with SUMO3 and SUMO5 (Fig. 5a,d). While the mutations (ORF4<sup>K78A</sup>, ORF4<sup>SIM2 Mut</sup> and ORF4<sup>SIM3 Mut</sup>) affecting the PD targeting ability of the ORF4 protein did not abolish the ORF4–SCE1/SUMO interaction, they did dramatically weaken it (Fig. 5b,e). We confirmed SUMOylation of the ORF4 protein using the *E. coli in vivo* SUMOylation assay, and the described mutations severely affected SUMOylation of the ORF4 protein (Fig. 5f). Downregulation of the mRNA levels of *NbSCE1* and *NbSUMO* significantly lowered the CMoV infection (Fig. 7d). These data suggest that the SUMOylation pathway plays an important role in regulating the PD targeting of the ORF4 protein. The infections of some animal viruses, such as Ebola virus, requires the SUMOylation system to enhance its replication (Vidal *et al.*, 2019). The SUMO modification also stabilizes the enterovirus 71 polymerase to facilitate the virus infection (Liu *et al.*, 2016). It is not well studied in the case of plant virus infections. So far, to the best of our knowledge, it has been shown that the SUMOylation components are required for virus infection for some potyviruses and geminiviruses (Sánchez-Durán *et al.*, 2011; Xiong & Wang, 2013). However, it is well known that the SUMOylation system is important for the plant development and stress tolerance (Morrell & Sadanandom, 2019). Thus, it is reasonable to



believe that more plant viruses hijack the SUMOylation components for their infection.

Our data demonstrate that the host SUMOylation system plays a pivotal role in CMoV infection; however, we do not know which cellular trafficking pathway the ORF4 protein follows to reach the PD. In the case of FMV, its MP translocates into the ER, and then reaches the ER–PM contact site or localizes to the microdomains of the PM, to further localize to the PD (Ishikawa *et al.*, 2017). For the CMoV ORF4 protein, no membrane-associated domain was predicted when the protein sequence was analyzed using multiple online prediction tools. However, we did find that a significant amount of ORF4 protein is membrane-associated (Fig. 2c). Furthermore, we found that the ORF4<sup>SIM2 Mut</sup>:GFP and ORF4<sup>SIM3 Mut</sup>:GFP are still cell wall-associated (Fig. 4c). It is possible that these mutated ORF4 proteins can still target PD, but to a lower degree. Another possibility is that the mutations of SIM2 and SIM3 cause the ORF4 protein to be retained at the unknown cell wall-associated microdomains. Thus, it will be interesting to explore further how the ORF4 protein targets the PD, and at which step of this process, the SUMOylation triggers the ORF4 protein to target the PD.

Finally, we extend what we found for CMoV to the ORF4 protein homologs of other umbraviruses. We found that residue K78 and the SIM2 were highly conserved among the *Umbravirus* ORF4 proteins (P27 in the case of PEMV2) (Fig. 8a). The mutation of the SIM2 motif also prevented the PEMV2 P27 protein from targeting the PD (Fig. 8b). Consequently, it is possible that other *Umbravirus* ORF4 proteins target the PD by interacting with host cell SUMOylation components.



## Acknowledgements

We are grateful to Dr Aiming Wang for the SUMO constructs. We thank Dr Savithamma Dinesh-Kumar for the TRV VIGS constructs, and Dr George Lomonosoff for the pEAQ-HT expression vector. We thank the laboratory members for critically reading the manuscript. This research was performed as part of a team supporting DARPA's Insect Allies Program. The views and conclusions contained in this document are those of the authors and should not be interpreted as representing the official policies, either expressed or implied, of DARPA or the US Government. The US Government is authorized to reproduce and distribute reprints for government purposes notwithstanding any copyright notation hereon.


## Author contributions


JJ, Y-WK and BWF designed the project; JJ carried out experiments with assistance from Y-WK, NS and AE; JJ and BWF wrote the manuscript. All authors reviewed and approved the manuscript.

## ORCID

Anna Erickson  <https://orcid.org/0000-0003-3937-9217>  
Bryce W. Falk  <https://orcid.org/0000-0002-5431-1627>

Jun Jiang  <https://orcid.org/0000-0002-6886-2331>

Yen-Wen Kuo  <https://orcid.org/0000-0003-2746-2953>

Nidà Salem  <https://orcid.org/0000-0003-3778-2213>

## References

- Angell SM, Davies C, Baulcombe DC. 1996. Cell-to-cell movement of potato virus X is associated with a change in the size-exclusion limit of plasmodesmata in trichome cells of *Nicotiana clelandii*. *Virology* 216: 197–201.
- Ashby J, Boutant E, Seemanpillai M, Sambade A, Ritzenthaler C, Heinlein M. 2006. Tobacco mosaic virus movement protein functions as a structural microtubule-associated protein. *Journal of Virology* 80: 8329–8344.
- Atkins D, Hull R, Wells B, Roberts K, Moore P, Beachy RN. 1991. The tobacco mosaic virus 30K movement protein in transgenic tobacco plants is localized to plasmodesmata. *Journal of General Virology* 72: 209–211.
- Augustine RC, Vierstra RD. 2018. SUMOylation: re-wiring the plant nucleus during stress and development. *Current Opinion in Plant Biology* 45: 143–154.
- Bachan S, Dinesh-Kumar SP. 2012. Tobacco rattle virus (TRV)-based virus-induced gene silencing. In: Watson JM, Wang M-B, eds. *Antiviral resistance in plants: methods and protocols*. Totowa, NJ, USA: Humana Press, 83–92.
- Beauchair G, Bridier-Nahmias A, Zagury J-F, Saïb A, Zamborlini A. 2015. JASSA: a comprehensive tool for prediction of SUMOylation sites and SIMs. *Bioinformatics* 31: 3483–3491.
- Brandner K, Sambade A, Boutant E, Didier P, Mély Y, Ritzenthaler C, Heinlein M. 2008. Tobacco mosaic virus movement protein interacts with green fluorescent protein-tagged microtubule end-binding protein 1. *Plant Physiology* 147: 611–623.
- Budhiraja R, Hermkes R, Müller S, Schmidt J, Colby T, Panigrahi K, Coupland G, Bachmair A. 2009. Substrates related to chromatin and to RNA-dependent processes are modified by Arabidopsis SUMO isoforms that differ in a conserved residue with influence on desumoylation. *Plant Physiology* 149: 1529–1540.
- Canetta E, Kim SH, Kalinina NO, Shaw J, Adya AK, Gillespie T, Brown JWS, Taliansky M. 2008. A plant virus movement protein forms ringlike complexes with the major nucleolar protein, fibrillarin, *in vitro*. *Journal of Molecular Biology* 376: 932–937.
- Cheng X, Xiong R, Li Y, Li F, Zhou X, Wang A. 2017. Sumoylation of Turnip mosaic virus RNA polymerase promotes viral infection by counteracting the host NPR1-mediated immune response. *The Plant Cell* 29: 508–525.
- Colby T, Matthäi A, Boeckelmann A, Stuible H-P. 2006. SUMO-conjugating and SUMO-deconjugating enzymes from Arabidopsis. *Plant Physiology* 142: 318–332.
- Demo CM, Oliver MJ, Beachy RN. 1987. The 30-kilodalton gene product of tobacco mosaic virus potentiates virus movement. *Science* 237: 389–394.
- Denecke J, De Rycke R, Botterman J. 1992. Plant and mammalian sorting signals for protein retention in the endoplasmic reticulum contain a conserved epitope. *EMBO Journal* 11: 2345–2355.
- Ding B, Li Q, Nguyen L, Palukaitis P, Lucas WJ. 1995. Cucumber mosaic virus 3a protein potentiates cell-to-cell trafficking of CMV RNA in tobacco plants. *Virology* 207: 345–353.
- Donald RG, Zhou H, Jackson AO. 1993. Serological analysis of barley stripe mosaic virus-encoded proteins in infected barley. *Virology* 195: 659–668.
- Gareau JR, Lima CD. 2010. The SUMO pathway: emerging mechanisms that shape specificity, conjugation and recognition. *Nature Reviews Molecular Cell Biology* 11: 861–871.
- Hu Y, Li Z, Yuan C, Jin X, Yan L, Zhao X, Zhang Y, Jackson AO, Wang X, Han C *et al.* 2015. Phosphorylation of TGB1 by protein kinase CK2 promotes barley stripe mosaic virus movement in monocots and dicots. *Journal of Experimental Botany* 66: 4733–4747.
- Ishikawa K, Hashimoto M, Yusa A, Koinuma H, Kitazawa Y, Netsu O, Yamaji Y, Namba S. 2017. Dual targeting of a virus movement protein to ER and plasma membrane subdomains is essential for plasmodesmata localization. *PLoS Pathogens* 13: e1006463.

- Kasteel DTJ, Perbal M-C, Boyer J-C, Wellink J, Goldbach RW, Maule AJ, van Lent JWM. 1996. The movement proteins of cowpea mosaic virus and cauliflower mosaic virus induce tubular structures in plant and insect cells. *Journal of General Virology* 77: 2857–2864.
- Kasteel DT, van der Wel NN, Jansen KA, Goldbach RW, van Lent JW. 1997. Tubule-forming capacity of the movement proteins of alfalfa mosaic virus and brome mosaic virus. *Journal of General Virology* 78: 2089–2093.
- Kato F, Hishiki T. 2016. Dengue virus reporter replicon is a valuable tool for antiviral drug discovery and analysis of virus replication mechanisms. *Viruses* 8: 122.
- Kato N, Sugiyama K, Namba K, Dansako H, Nakamura T, Takami M, Naka K, Nozaki A, Shimotohno K. 2003. Establishment of a hepatitis C virus subgenomic replicon derived from human hepatocytes infected *in vitro*. *Biochemical and Biophysical Research Communications* 306: 756–766.
- Kawakami S, Watanabe Y, Beachy RN. 2004. Tobacco mosaic virus infection spreads cell to cell as intact replication complexes. *Proceedings of the National Academy of Sciences, USA* 101: 6291–6296.
- Kerscher O. 2007. SUMO junction—what's your function? *EMBO Reports* 8: 550–555.
- Kim SH, MacFarlane S, Kalinina NO, Rakitina DV, Ryabov EV, Gillespie T, Haupt S, Brown JWS, Taliansky M. 2007a. Interaction of a plant virus-encoded protein with the major nucleolar protein fibrillarin is required for systemic virus infection. *Proceedings of the National Academy of Sciences, USA* 104: 11115–11120.
- Kim SH, Ryabov EV, Kalinina NO, Rakitina DV, Gillespie T, MacFarlane S, Haupt S, Brown JW, Taliansky M. 2007b. Cajal bodies and the nucleolus are required for a plant virus systemic infection. *EMBO Journal* 26: 2169–2179.
- Laporte C, Vetter G, Loudes A-M, Robinson DG, Hillmer S, Stussi-Graud C, Ritzenthaler C. 2003. Involvement of the secretory pathway and the cytoskeleton in intracellular targeting and tubule assembly of Grapevine fanleaf virus movement protein in tobacco BY-2 cells. *The Plant Cell* 15: 2058–2075.
- Liu Y, Zheng Z, Shu B, Meng J, Zhang Y, Zheng C, Ke X, Gong P, Hu Q, Wang H. 2016. SUMO modification stabilizes enterovirus 71 polymerase 3D to facilitate viral replication. *Journal of Virology* 90: 10472–10485.
- Morrell R, Sadanandom A. 2019. Dealing with stress: a review of plant SUMO proteases. *Frontiers in Plant Science* 10: 19.
- Nurkiyanova KM, Ryabov EV, Kalinina NO, Fan Y, Andreev I, Fitzgerald AG, Palukaitis P, Taliansky M. 2001. Umbravirus-encoded movement protein induces tubule formation on the surface of protoplasts and binds RNA incompletely and non-cooperatively. *Journal of General Virology* 82: 2579–2588.
- Okada S, Nagabuchi M, Takamura Y, Nakagawa T, Shinmyozu K, Nakayama J-i, Tanaka K. 2009. Reconstitution of *Arabidopsis thaliana* SUMO pathways in *E. coli*: functional evaluation of SUMO machinery proteins and mapping of SUMOylation sites by mass spectrometry. *Plant and Cell Physiology* 50: 1049–1061.
- Qiao W, Medina V, Kuo Y-W, Falk BW. 2018. A distinct, non-virion plant virus movement protein encoded by a Crinivirus essential for systemic infection. *MBio* 9: e02230–e2218.
- Robles Luna G, Peña EJ, Borniego MB, Heinlein M, García ML. 2018. Citrus Psorosis virus movement protein contains an aspartic protease required for autocleavage and the formation of tubule-like structures at plasmodesmata. *Journal of Virology* 92: e00355–e01318.
- Ryabov EV, Oparka KJ, Santa Cruz S, Robinson DJ, Taliansky ME. 1998. Intracellular location of two groundnut rosette umbravirus proteins delivered by PVX and TMV vectors. *Virology* 242: 303–313.
- Ryabov EV, Roberts IM, Palukaitis P, Taliansky M. 1999. Host-specific cell-to-cell and long-distance movements of cucumber mosaic virus are facilitated by the movement protein of groundnut rosette virus. *Virology* 260: 98–108.
- Ryabov EV, Robinson DJ, Taliansky ME. 1999. A plant virus-encoded protein facilitates long-distance movement of heterologous viral RNA. *Proceedings of the National Academy of Sciences, USA* 96: 1212–1217.
- Sainsbury F, Thuenemann EC, Lomonosoff GP. 2009. pEAQ: versatile expression vectors for easy and quick transient expression of heterologous proteins in plants. *Plant Biotechnology Journal* 7: 682–693.
- Saint-Jore CM, Evins J, Batoko H, Brandizzi F, Moore I, Hawes C. 2002. Redistribution of membrane proteins between the Golgi apparatus and endoplasmic reticulum in plants is reversible and not dependent on cytoskeletal networks. *The Plant Journal* 29: 661–678.
- Sakulkoo W, Osés-Ruiz M, Oliveira Garcia E, Soanes DM, Littlejohn GR, Hacker C, Correia A, Valent B, Talbot NJ. 2018. A single fungal MAP kinase controls plant cell-to-cell invasion by the rice blast fungus. *Science* 359: 1399–1403.
- Sánchez-Durán MA, Dallas MB, Ascencio-Ibañez JT, Reyes MI, Arroyo-Mateos M, Ruiz-Albert J, Hanley-Bowdoin L, Bejarano ER. 2011. Interaction between Geminivirus replication protein and the SUMO-conjugating enzyme is required for viral infection. *Journal of Virology* 85: 9789–9800.
- Saracco SA, Miller MJ, Kurepa J, Vierstra RD. 2007. Genetic analysis of SUMOylation in Arabidopsis: conjugation of SUMO1 and SUMO2 to nuclear proteins is essential. *Plant Physiology* 145: 119–134.
- Sparkes IA, Runions J, Kearns A, Hawes C. 2006. Rapid, transient expression of fluorescent fusion proteins in tobacco plants and generation of stably transformed plants. *Nature Protocols* 1: 2019–2025.
- Su S, Liu Z, Chen C, Zhang Y, Wang X, Zhu L, Miao L, Wang X-C, Yuan M. 2010. Cucumber mosaic virus movement protein severs actin filaments to increase the plasmodesmal size exclusion limit in tobacco. *The Plant Cell* 22: 1373–1387.
- Taliansky M, Roberts IM, Kalinina N, Ryabov EV, Raj SK, Robinson DJ, Oparka KJ. 2003. An umbravirus protein, involved in long-distance RNA movement, binds viral RNA and forms unique, protective ribonucleoprotein complexes. *Journal of Virology* 77: 3031–3040.
- Tilsner J, Linnik O, Wright KM, Bell K, Roberts AG, Lacomme C, Santa Cruz S, Oparka KJ. 2012. The TGB1 Movement protein of potato virus X reorganizes actin and endomembranes into the X-body, a viral replication factory. *Plant Physiology* 158: 1359–1370.
- Tilsner J, Linnik O, Louveaux M, Roberts IM, Chapman SN, Oparka KJ. 2013. Replication and trafficking of a plant virus are coupled at the entrances of plasmodesmata. *Journal of Cell Biology* 201: 981–995.
- Vaquero C, Turner AP, Demangeat G, Sanz A, Serra MT, Roberts K, García-Luque I. 1994. The 3a protein from cucumber mosaic virus increases the gating capacity of plasmodesmata in transgenic tobacco plants. *Journal of General Virology* 75: 3193–3197.
- Vidal S, El Motiam A, Seoane R, Preitakaite V, Bouzaher YH, Gómez-Medina S, San Martín C, Rodríguez D, Rejas MT, Baz-Martínez M *et al.* 2019. Regulation of the Ebola Virus VP24 Protein by SUMO. *Journal of Virology* 94: e01687–e1619.
- Waigmann E, Chen M-H, Bachmaier R, Ghoshroy S, Citovsky V. 2000. Regulation of plasmodesmal transport by phosphorylation of tobacco mosaic virus cell-to-cell movement protein. *EMBO Journal* 19: 4875–4884.
- Wellink J, van Lent JW, Verver J, Sijen T, Goldbach RW, van Kammen A. 1993. The cowpea mosaic virus M RNA-encoded 48-kilodalton protein is responsible for induction of tubular structures in protoplasts. *Journal of Virology* 67: 3660–3664.
- Wilson VG, Rangasamy D. 2001. Intracellular targeting of proteins by sumoylation. *Experimental Cell Research* 271: 57–65.
- Wolf S, Lucas WJ, Deom CM, Beachy RN. 1989. Movement protein of tobacco mosaic virus modifies plasmodesmal size exclusion limit. *Science* 246: 377–379.
- Xiong R, Wang A. 2013. SCE1, the SUMO-conjugating enzyme in plants that interacts with Nib, the RNA-dependent RNA polymerase of Turnip mosaic virus, is required for viral infection. *Journal of Virology* 87: 4704–4715.
- Yuan C, Lazarowitz SG, Citovsky V. 2018. The plasmodesmal localization signal of TMV MP is recognized by plant synaptotagmin SYTA. *MBio* 9: e01314–01318.
- Zhao Q, Xie Y, Zheng Y, Jiang S, Liu W, Mu W, Liu Z, Zhao Y, Xue Y, Ren J. 2014. GPS-SUMO: a tool for the prediction of sumoylation sites and SUMO-interaction motifs. *Nucleic Acids Research* 42(W1): W325–W330.

## Supporting Information

Additional Supporting Information may be found online in the Supporting Information section at the end of the article.

**Fig. S1** Characterization of the ORF3:GFP protein and its mutated protein fusions.

**Fig. S2** RT-PCR detection of CMoV vRNA accumulation in the upper noninoculated leaf tissues of *N. benthamiana* and *A. thaliana* plants.

**Methods S1** Additional Materials and Methods information.

**Table S1** Primers used in this study.

Please note: Wiley Blackwell are not responsible for the content or functionality of any Supporting Information supplied by the authors. Any queries (other than missing material) should be directed to the *New Phytologist* Central Office.



### About *New Phytologist*

- *New Phytologist* is an electronic (online-only) journal owned by the New Phytologist Foundation, a **not-for-profit organization** dedicated to the promotion of plant science, facilitating projects from symposia to free access for our Tansley reviews and Tansley insights.
- Regular papers, Letters, Viewpoints, Research reviews, Rapid reports and both Modelling/Theory and Methods papers are encouraged. We are committed to rapid processing, from online submission through to publication 'as ready' via *Early View* – our average time to decision is <26 days. There are **no page or colour charges** and a PDF version will be provided for each article.
- The journal is available online at Wiley Online Library. Visit **www.newphytologist.com** to search the articles and register for table of contents email alerts.
- If you have any questions, do get in touch with Central Office (np-centraloffice@lancaster.ac.uk) or, if it is more convenient, our USA Office (np-usaoffice@lancaster.ac.uk)
- For submission instructions, subscription and all the latest information visit **www.newphytologist.com**